Secure finite-time event-triggered control for Markov jump systems under multiple cyber attacks

Jin Ok Baek[a], Ju H. Park[a,*], Yang Gu[a,b,*]

[a]*Department of Electrical Engineering, Yeungnam University, 280 Daehak-Ro, Kyongsan 38541, Republic of Korea*
[b]*School of Mechanical and Power Engineering, Nanjing Tech University, Nanjing, 211816, China*

Abstract

This paper investigates a dynamic event-triggered secure finite-time control strategy for networked Markov jump systems subjected to multiple cyber attacks. To characterize the stochastic nature of these cyber attacks, a probabilistic model incorporating two Bernoulli-distributed variables is employed. A dynamic event-triggered mechanism, designed with a triggering threshold structured as a diagonal matrix, is developed to reduce the frequency of communication. Leveraging Lyapunov stability theory and a structured separation technique, sufficient conditions are established to ensure the stochastic finite-time boundedness of the closed-loop system while achieving a prescribed H_2-gain performance. Furthermore, comparative simulations are conducted to validate the effectiveness and practical advantages of the proposed approach.

Keywords: Stochastic finite-time boundedness, finite-time H_2-gain, event-triggered scheme, internal dynamic function, DoS attacks, deception attacks

1. Introduction

In control theory, a wide range of approaches from classical techniques to modern methods has been developed to achieve the stabilization of systems. Among classical methods, proportional-integral-derivative (PID) control remains one of the most widely used due to its simplicity and effectiveness. Modern control approaches such as the linear quadratic regulator and linear quadratic Gaussian control focus on optimizing system performance. Additionally, model predictive control [1], H_∞ robust control [2], and other advanced approaches have been introduced to enhance stability and robustness in the presence of disturbances and uncertainties. Beyond these, more sophisticated strategies such as PI controller tuning via data-driven algorithms [3], sliding mode control [4], [5], and adaptive control [6] have been proposed to address nonlinearities and time-varying dynamics. Furthermore, intelligent control methods including fuzzy logic control [7], neural network control [8], reinforcement learning-based control [9], and hybrid control [10] have further improved adaptability and decision-making capabilities in complex systems.

Networked control systems (NCSs) have been widely applied in various fields, including industrial automation, smart grids, autonomous vehicles, and cyber-physical systems. There are several different data transmission methods in NCSs, among which the time-triggered scheme and the event-triggered scheme (ETS) are commonly used [11]. The time-triggered scheme refers to a communication strategy in which data transmissions occur at pre-determined fixed time intervals. While this method ensures regular updates, it may lead to inefficient use of communication resources due to unnecessary transmissions. In contrast, ETS initiates data transmission only when certain event-triggering conditions are violated, thereby significantly reducing the number of triggering times between the sensor and the controller [12]. ETS has attracted much attention in recent years due to its advantage in increasing communication efficiency and

*Corresponding authors.
Email addresses: jbaek0125@yu.ac.kr (Jin Ok Baek), jessie@ynu.ac.kr (Ju H. Park), yanggu@njtech.edu.cn (Yang Gu)

reducing network load. A dual channel ETS and a corresponding composite controller were suggested in [13] for linear systems to ensure that the system is uniformly ultimately bounded. An enhanced ETS with designable inter-event times was proposed in [14] for intelligent vehicles under bounded disturbances. [15] tackled the issue of event-triggered asynchronous control and strict dissipativity for a discrete-time Markov jump system (MJS) affected by mismatched modes and unpredictable parameter uncertainties. In [16], a dynamic event-triggered sliding mode control approach was developed for repeated scalar nonlinear systems to achieve asymptotic stability with specified H_∞ performance. [17] designed an adaptive event-triggered asynchronous state-feedback controller such that the closed-loop system is finite-time bounded with a certain level of dissipative performance.

Another critical issue facing NCSs is cyber security, which is becoming increasingly significant due to the growing openness of communication networks and the advancement of cyber attack techniques. Cyber attacks can significantly disrupt system operations, so it is important to address these cyber attacks carefully. There are several kinds of cyber attacks such as replay attacks, deception attacks and denial-of-service (DoS) attacks. Recently, many researchers have studied the security issues of systems subject to cyber attacks. [18] adopted a hybrid-triggering scheme consisting of time-triggered scheme and ETS to ensure the asymptotic stability of system under cyber attacks. [19] studied the output-based resilient event-triggered control for NCSs subject to DoS attacks. [20] introduced relaxed linear matrix inequality (LMI) design conditions supported by a suitable Lyapunov-Krasovskii functional to ensure system stability under deception attacks. [21] explored an observer-based resilient ETS for networked linear systems affected by periodic DoS jamming attacks. In [22], an adaptive event-triggered state-feedback control approach based on neural networks was designed for resource-constrained cyber-physical systems to alleviate the impact of several cyber attacks. [23] established a non-fragile output-feedback controller (OFC) with a compensation component to achieve stochastic stability with strict dissipative performance.

On another research front, finite-time stability and finite-time boundedness (FTB) have also received much attention over the past few decades. Conventional control approaches typically aim for asymptotic stability, where the system eventually converges to an equilibrium point over an infinite time. While such asymptotic stability is effective in many scenarios, it may not be suitable for time-critical applications, where rapid stabilization is essential. In this context, FTB stabilization offers a more practical alternative by ensuring that the system remains stable for a finite and predetermined time. FTB stabilization is particularly suitable for practical systems such as robotics and aircraft engine control, where fast response and robustness are critical. A considerable number of studies have addressed finite-time stability, including the following: In [24], the finite-time generalized H_2 norm was defined, which is the same concept as the finite-time H_2-gain defined in this paper, and represents the supremum of the ratio of the output to the combined energy of the external disturbance and the nonzero initial state over a finite-time interval. Finite-time stability of the system was investigated in [25] using a state-feedback controller. FTB was studied in [26] for both linear time-invariant systems and time-varying systems under finite-time H_2-gain performance constraints. [27] addressed the problem of finite-time stabilization for a class of uncertain Hamiltonian systems via sliding mode control.

There are many reported results in the design of controllers that guarantee system stability with H_∞ performance. However, research on designing stabilizing controllers that meet finite-time H_2-gain performance is relatively scarce, which serves as the motivation for this study. In particular, designing secure finite-time H_2 static/dynamic OFC for MJS with an event-triggered framework, especially in the presence of cyber attacks, remains an important problem. In our previous work [28], we investigated FTB stabilization of MJS in the absence of cyber attacks by designing an ETS and a state-feedback controller. In this study, we extend our approach by designing an ETS and an OFC to achieve FTB stabilization with H_2 performance of MJS under multiple cyber attacks. The contributions of this study are the following:

(i) Finite-time H_2-gain performance: We designed a dynamic ETS-based static/dynamic OFC to ensure that the system meets the finite-time H_2-gain performance index γ rather than H_∞ performance.

(ii) General dynamic ETS: A general dynamic ETS with a diagonal triggering threshold is provided to further reduce frequency of communication. This ETS can be simplified to the existing static [11], specific dynamic ETS [12].

(iii) Structured separation technique: To handle coupling terms, a structured separation technique is

employed in this paper. This technique transforms matrix inequalities into tractable LMIs using auxiliary variable matrices.

Notations: $\mathbb{R}^n$ is the n-dimensional Euclidean space. $\mathbb{M}_{m\times n}(\mathbb{R})$ is the set of $m \times n$ real matrices, simply denote $\mathbb{M}_{m\times n}$. Denote I as the identity matrix and $\mathbb{N}_0$ as the set of positive integers including zero. $M > 0 (M \geq 0)$ and $M < 0 (M \leq 0)$ signify that M is a positive-definite(positive semi-definite) and a negative-definite(negative semi-definite) matrix, respectively. $M^\top$ is the transpose of M and $*$ means the entry in the symmetric position of a symmetric matrix after transposition. $He(M)$ stands for $M + M^\top$. $\mathcal{E}$ is mathematical expectation and Pr denotes the probability. For a vector $b(t)$, $\|b(t)\| := \sqrt{b^\top(t)b(t)}$. $\|b(t)\|_{L_\infty,[0,T]} := esssup_{t\in[0,T]}\|b(t)\|$ and $\|b(t)\|_{L_2,[0,T]} := \left(\int_0^T \|b(t)\|^2 dt\right)^{\frac{1}{2}}$ represent finite-time L_∞-norm and finite-time L_2-norm of $b(t)$, respectively. And diag $\{\cdots\}$ is a diagonal matrix.

2. Foundations and Description of Problem

Consider the continuous-time MJS given by

$$\begin{cases} \dot{x}(t) = A(r_t)x(t) + B(r_t)\mathfrak{u}(t) + D(r_t)w(t), \\ y(t) = C(r_t)x(t) \quad \text{with initial state } x(0) \text{ at } t = 0, \end{cases} \tag{1}$$

where $x(t) \in \mathbb{R}^{n_x}$, $\mathfrak{u}(t) \in \mathbb{R}^{n_u}$, $y(t) \in \mathbb{R}^{n_y}$ refer to the system state, control input and measured output vector, respectively; $w(t) \in \mathbb{R}^{n_d}$ is the external disturbance in the space $L_2[0,T]$. $A(r_t) \in \mathbb{M}_{n_x\times n_x}$, $B(r_t) \in \mathbb{M}_{n_x\times n_u}$, $C(r_t) \in \mathbb{M}_{n_y\times n_x}$ and $D(r_t) \in \mathbb{M}_{n_x\times n_d}$ are known system matrices. Here, $\{r_t\}_{t\geq 0}$ is Markov process, and each r_t belongs to the set $S_1 = \{1, 2, \cdots, s_1\}$. For any modes of the MJS, the transition rate matrix (TRM) is $\Pi = [\pi_{ij}]_{i,j=1}^{s_1}$ with

$$Pr(r_{t+\Delta t} = j \mid r_t = i) = \delta_{ij} + \pi_{ij}\ \Delta t + o(\Delta t),$$

where δ_{ij} is the Kronecker delta and $\Delta t > 0$. $\lim_{\Delta t\to 0} o(\Delta t)/\Delta t = 0$, and π_{ij} signifies the rate at which the system shifts from mode i at time t to mode j at time $t + \Delta t$ with $\pi_{ij} \geq 0$ for all $j \neq i$, and $\pi_{ii} = -\sum_{j=1,j\neq i}^{s_1} \pi_{ij}$. For $r_t = i \in S_1$, we abbreviate $A(r_t)$, $B(r_t)$, $C(r_t)$ and $D(r_t)$ as A_i, B_i, C_i and D_i, respectively.

Assumption 1. *Let $[0,T]$ be a time interval, $c_1 > 0$ be scalar, $\mathcal{R}$ be a $n_x \times n_x$ symmetric positive-definite matrix. Suppose that the initial state $x(0)$ satisfies $x^\top(0)\mathcal{R}x(0) \leq c_1$.*

Assumption 2. *For a given positive scalar d, the external disturbance $w(t)$ satisfies $\int_0^T w^\top(t)w(t)dt \leq d$.*

Assumption 3. *[30] Let $\kappa_d(t)$ and $\kappa_c(t)$ are Bernoulli-distributed random variables that indicate whether DoS attacks and deception attacks occur, respectively. Suppose that $\kappa_d(t)$ and $\kappa_c(t)$ are independent and their expectation values are $\mathcal{E}[\kappa_d(t)] = Pr(\kappa_d(t) = 1) = \overline{\kappa}_d$, $\mathcal{E}[\kappa_c(t)] = Pr(\kappa_c(t) = 1) = \overline{\kappa}_c$.*

Assumption 4. *[31] For a given positive scalar ρ, the deception attack signal $g(t)$ satisfies*

$$\|g(t)\|^2 \leq \rho\|x(t)\|^2, \qquad t \in [t_k, t_{k+1}) \subset [0,T].$$

Definition 1. *[32] Let $[0,T]$ be a time interval. Under Assumption 1 and Assumption 2, the system (1) is said to be stochastically FTB with respect to $(c_1, c_2, \mathcal{R}, T, d)$ if there exist a scalar c_2 with $c_1 < c_2$ such that $\mathcal{E}[x^\top(t)\mathcal{R}x(t)] < c_2$ for all $t \in [0,T]$.*

Definition 2. *[26] Given a finite-time interval $[0,T]$ and a $n_x \times n_x$ matrix $E_0^\top = E_0 > 0$, the finite-time H_2-gain for the system (1) is*

$$J((1), E_0, T) := sup_{w(t),x(0)} \Big(\frac{\|y(t)\|^2_{L_\infty,[0,T]}}{\|w(t)\|^2_{L_2,[0,T]} + x^\top(0) E_0 x(0)} \Big)^{\frac{1}{2}},$$

where $\|w(t)\|^2_{L_2,[0,T]} + x^\top(0)E_0x(0) \neq 0$. The system (1) meets the finite-time H_2-gain performance index γ if there exist a positive scalar γ such that $J((1), E_0, T) < \gamma$.

Lemma 1. *(Finsler's Lemma) Let $x \in \mathbb{R}^n$, $\mathcal{G}^\top = \mathcal{G} \in \mathbb{R}^{n\times n}$, $\mathcal{D} \in \mathbb{R}^{m\times n}$ with rank$(\mathcal{D}) < n$. The following statements are equivalent:*

1) $x^\top \mathcal{G} x < 0$ for all $\mathcal{D}x = 0$, $x \neq 0$.

2) $\exists\ \mathcal{X} \in \mathbb{R}^{n\times m}$ such that $\mathcal{G} + He(\mathcal{X}\mathcal{D}) < 0$.

3) $\mathcal{D}^{\perp\top} \mathcal{G} \mathcal{D}^\perp < 0$.

4) $\exists\ \mu \in \mathbb{R}$ such that $\mathcal{G} - \mu \mathcal{D}^\top \mathcal{D} < 0$.

2.1. Dynamic ETS design

Firstly, we define the measurement error $e(t) := y(t_k) - y(t),\ t \in [t_k, t_{k+1}) \subset [0,T]$, where $\{t_k\}_{k\in\mathbb{N}_0}$ is the sequence of triggering time instants with $t_0 = 0$. In order to construct a dynamic ETS, we propose a mode-independent internal dynamic function $\mathfrak{y}(t) > 0$ satisfying

$$\dot{\mathfrak{y}}(t) = -\lambda \mathfrak{y}(t) + y^\top(t_k)\widetilde{D}\widetilde{\Omega} y(t_k) - e^\top(t)\widetilde{\Omega} e(t),$$

where $\lambda > 0$, weighting matrix $\widetilde{\Omega}^\top = \widetilde{\Omega} > 0$ and triggering threshold $\widetilde{D} := \text{diag}\{d_1(t), d_2(t), \cdots d_{n_y}(t)\}$ with $d_j(t)$ satisfying $0 \leq d_j(t) \leq 1$ for all $j = 1, 2, \cdots, n_y$.

Then, let us consider a dynamic ETS defined by the following rule: $t_0 = 0$;

$$t_{k+1} = \inf\{t \in \mathbb{R} \mid t > t_k,\ \ \frac{1}{\theta}(\ \mathfrak{y}(t) + y^\top(t_k)\widetilde{D}\widetilde{\Omega} y(t_k) - e^\top(t)\widetilde{\Omega} e(t)\ ) \leq 0\}, \tag{2}$$

where t_{k+1} is the next triggering time instant.

Problem 1. *(FTB Stabilization Problem) For given scalars $c_1 > 0, d > 0$, $\theta > 1$ and matrix $R^\top = R > 0$, design an OFC $\mathfrak{u}(t) = \mathfrak{u}(t_k)$ for $t \in [t_k, t_{k+1})$ under the event-triggered rule in (2) such that the closed-loop system is stochastically FTB with respect to (c_1, c_2, R, T, d) and the system meets the finite-time H_2-gain performance index γ.*

2.2. Multiple cyber attacks modeling

A multiple cyber attacks' model to represent their random nature is established as follows:

$$y_a(t) := (1 - \kappa_d(t))[(1 - \kappa_c(t))y(t_k) + \kappa_c(t) g(t)], \tag{3}$$

where $g(t)$ is a deception attack signal.

Remark 1. *The general dynamic ETS in (2) in this paper offers a unified framework that covers several special cases:*

1) When $\mathfrak{y}(t) \neq 0$ and all diagonal elements in the threshold matrix $\widetilde{D}$ are the same scalar σ, the $\widetilde{D}$ is converted to σI, the ETS (2) becomes a specific dynamic ETS in [12].

2) When $\mathfrak{y}(t) \neq 0$ and all diagonal elements in $\widetilde{D}$ are the same time-varying function $\sigma(t)$, the ETS (2) becomes an adaptive dynamic ETS in [22].

3) When $\mathfrak{y}(t) = 0$ and all diagonal elements in the threshold matrix $\widetilde{D}$ are the same scalar σ, the ETS (2) becomes a static ETS in [11].

4) When $\mathfrak{y}(t) = 0$ and $\widetilde{D}$ approaches 0, the ETS (2) aggravates into a time-triggered scheme.

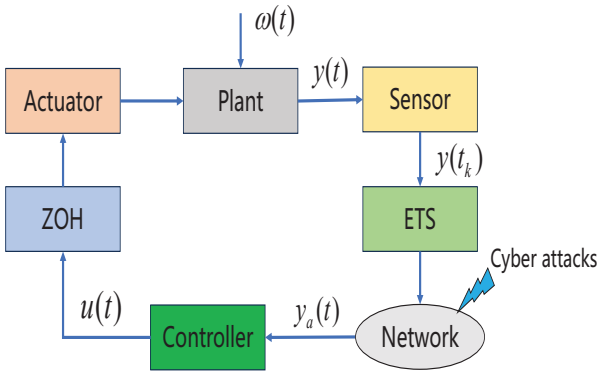

Figure 1: Block diagram of event-triggered NCSs impacted by multiple cyber attacks.

3. Main Results

This section addresses the secure FTB problem for the dynamic event-triggered MJS by designing a static/dynamic OFC under multiple cyber attacks.

3.1. Static OFC design under the dynamic ETS

In consideration of the multiple cyber attacks, we design a mode-dependent static OFC

$$\mathfrak{u}(t) = K(r_t)y_a(t), \qquad t \in [t_k, t_{k+1}), \tag{4}$$

where $K(r_t)$ is the controller gain matrix that needs to be designed.
Substituting (4) into the system (1) with $r_t = i$, we have a closed-loop system that takes the form:

$$\begin{cases} \dot{x}(t) = (A_i + (1-\kappa_d(t))(1-\kappa_c(t))B_iK_iC_i)x(t) + (1-\kappa_d(t))(1-\kappa_c(t))B_iK_ie(t) \\ \qquad\qquad +(1-\kappa_d(t))\kappa_c(t)B_iK_ig(t) + D_iw(t), \\ y(t) = C_ix(t), \qquad t \in [t_k, t_{k+1}) \subset [0, T]. \end{cases} \tag{5}$$

Based on the static OFC under the dynamic ETS and the multiple cyber attacks, Problem 1 can be solved for the system (5) in Theorem 1.

Theorem 1. *Let $\alpha > 0, d > 0, T > 0$, $a_1 > 0, \rho > 0$, $c_1 > 0$ and $\lambda > 0$ with $\lambda > \frac{1}{\theta}$. Suppose that Assumptions 1 - 4 hold, and $\mathfrak{y}(0) = \phi x^\top(0)x(0)$ for a scalar $\phi > 0$. If there exist $P_i^\top = P_i > 0$, $\widetilde{\Omega}^\top = \widetilde{\Omega} > 0$, matrices V_i, W_i and scalars $\gamma > 0$, $\beta > 1$, $c_2 > 0$ with $c_1 < c_2$ such that*

$$\begin{bmatrix} \Gamma_{11} & \Gamma_{12} & P_iD_i & \Gamma_{14} & \Gamma_{15} \\ * & \Gamma_{22} & 0 & 0 & \Gamma_{25} \\ * & * & -I & 0 & 0 \\ * & * & * & -I & \Gamma_{45} \\ * & * & * & * & \Gamma_{55} \end{bmatrix} < 0, \tag{6}$$

$$\mathcal{R} < P_i < \beta\mathcal{R}, \tag{7}$$

$$e^{\alpha T}(\beta c_1 + d + \mathfrak{y}(0)) < c_2, \tag{8}$$

$$\frac{1}{\gamma^2}C_i^\top C_i \le P_i \le E_0 - \phi I \tag{9}$$

for all $i \in S_1$, where

$$\Gamma_{11} = He(P_iA_i + a_1(1-\overline{\kappa}_d)(1-\overline{\kappa}_c)B_iW_iC_i) + \rho I + \sum_{m=1}^{s_1}\pi_{im}P_m - \alpha P_i + (1+\frac{1}{\theta})C_i^\top \widetilde{D}\widetilde{\Omega}C_i,$$

$$\Gamma_{12} = a_1(1-\overline{\kappa}_d)(1-\overline{\kappa}_c)B_iW_i + (1+\frac{1}{\theta})C_i^\top \widetilde{D}\widetilde{\Omega}, \qquad \Gamma_{14} = a_1(1-\overline{\kappa}_d)\overline{\kappa}_cB_iW_i,$$

$$\Gamma_{15} = P_iB_i - a_1B_iV_i + a_1(1-\overline{\kappa}_d)(1-\overline{\kappa}_c)C_i^\top W_i^\top, \qquad \Gamma_{22} = -(1+\frac{1}{\theta})(I-\widetilde{D})\widetilde{\Omega},$$

$$\Gamma_{25} = a_1(1-\overline{\kappa}_d)(1-\overline{\kappa}_c)W_i^\top, \qquad \Gamma_{45} = a_1(1-\overline{\kappa}_d)\overline{\kappa}_cW_i^\top, \qquad \Gamma_{55} = -a_1He(V_i),$$

and $\mathcal{R}^\top = \mathcal{R} > 0$, $E_0^\top = E_0 > 0$, then Problem 1 is solved by designing the mode-dependent static OFC (4), that is, the closed-loop system (5) is stochastically FTB with finite-time H_2-gain performance index γ. Additionally, K_i can be solved by $K_i = V_i^{-1}W_i$.

Proof. For each fixed $r_t = i \in S_1$, the stochastic Lyapunov function is selected as

$$V(x(t), i) = x^\top(t)P_ix(t) + \mathfrak{y}(t)$$

with $P_i^\top = P_i > 0$.
By taking the weak infinitesimal operator $\mathcal{I}$, we have

$$\mathcal{E}[\mathcal{I}(V(x(t),i))] = \mathcal{E}[\dot{x}^\top(t)P_ix(t) + x^\top(t)P_i\dot{x}(t) + x^\top(t)(\sum_{m=1}^{s_1}\pi_{im}P_m)x(t) + \dot{\mathfrak{y}}(t)].$$

From the system (5) and the derivative of $\mathfrak{y}(t)$, it leads to

$$\begin{aligned}\mathcal{E}[\mathcal{I}(V(x(t),i))] =& x^\top(t)\{He(P_i(A_i + (1-\overline{\kappa}_d)(1-\overline{\kappa}_c)B_iK_iC_i)) + \sum_{m=1}^{s_1}\pi_{im}P_m\}x(t)\\ &+ (1-\overline{\kappa}_d)(1-\overline{\kappa}_c)x^\top(t)P_iB_iK_ie(t) + (1-\overline{\kappa}_d)(1-\overline{\kappa}_c)e^\top(t)K_i^\top B_i^\top P_ix(t)\\ &+ (1-\overline{\kappa}_d)\overline{\kappa}_cx^\top(t)P_iB_iK_ig(t) + (1-\overline{\kappa}_d)\overline{\kappa}_cg^\top(t)K_i^\top B_i^\top P_ix(t) + x^\top(t)P_iD_iw(t)\\ &+ w^\top(t)D_i^\top P_ix(t) - \lambda\mathfrak{y}(t) + y^\top(t_k)\widetilde{D}\widetilde{\Omega}y(t_k) - e^\top(t)\widetilde{\Omega}e(t).\end{aligned}$$

Combining the event-triggering condition $\frac{1}{\theta}(\mathfrak{y}(t) + y^\top(t_k)\widetilde{D}\widetilde{\Omega}y(t_k) - e^\top(t)\widetilde{\Omega}e(t)) \geq 0$, Assumption 4 and $(\frac{1}{\theta} - \lambda)\mathfrak{y}(t) < 0$, the following inequality is obtained:

$$\begin{aligned}\mathcal{E}[\mathcal{I}(V(x(t),i))] <& x^\top(t)\{He(P_i(A_i + (1-\overline{\kappa}_d)(1-\overline{\kappa}_c)B_iK_iC_i)) + \sum_{m=1}^{s_1}\pi_{im}P_m + \rho I + (1+\frac{1}{\theta})C_i^\top\widetilde{D}\widetilde{\Omega}C_i\}x(t)\\ &+ x^\top(t)((1-\overline{\kappa}_d)(1-\overline{\kappa}_c)P_iB_iK_i + (1+\frac{1}{\theta})C_i^\top\widetilde{D}\widetilde{\Omega})e(t) + x^\top(t)P_iD_iw(t)\\ &+ e^\top(t)((1-\overline{\kappa}_d)(1-\overline{\kappa}_c)K_i^\top B_i^\top P_i + (1+\frac{1}{\theta})\widetilde{D}\widetilde{\Omega}C_i)x(t) + w^\top(t)D_i^\top P_ix(t)\\ &+ (1-\overline{\kappa}_d)\overline{\kappa}_cx^\top(t)P_iB_iK_ig(t) + (1-\overline{\kappa}_d)\overline{\kappa}_cg^\top(t)K_i^\top B_i^\top P_ix(t)\\ &- (1+\frac{1}{\theta})e^\top(t)(I-\widetilde{D})\widetilde{\Omega}e(t) - g(t)^\top g(t).\end{aligned}$$

That is,

$$\mathcal{E}[\mathcal{I}(V(x(t),i))] < \xi^\top(t)\begin{bmatrix}\Phi_{11} & \Phi_{12} & P_iD_i & \Phi_{14}\\ * & \Gamma_{22} & 0 & 0\\ * & * & 0 & 0\\ * & * & * & -I\end{bmatrix}\xi(t), \tag{10}$$

where $\xi^\top(t) := [x^\top(t)\ e^\top(t)\ w^\top(t)\ g^\top(t)]$, $\Phi_{11} = He(P_i(A_i + (1-\overline{\kappa}_d)(1-\overline{\kappa}_c)B_iK_iC_i)) + \sum_{m=1}^{s_1}\pi_{im}P_m + \rho I + (1+\frac{1}{\theta})C_i^\top \widetilde{D}\widetilde{\Omega}C_i$, $\Phi_{12} = (1-\overline{\kappa}_d)(1-\overline{\kappa}_c)P_iB_iK_i + (1+\frac{1}{\theta})C_i^\top\widetilde{D}\widetilde{\Omega}$ and $\Phi_{14} = (1-\overline{\kappa}_d)\overline{\kappa}_cP_iB_iK_i$. Define

$$J_1 := \mathcal{E}[\mathcal{I}(V(x(t),i)) - \alpha V(x(t),i) - w^\top(t)w(t)].$$

Since $\alpha > 0, \mathfrak{y}(t) > 0$ for all $t \in [t_k, t_{k+1}) \subset [0,T]$ and based on (10), J_1 yields

$$J_1 < \xi^\top(t)\begin{bmatrix}\Phi_{11}-\alpha P_i & \Phi_{12} & P_iD_i & \Phi_{14}\\ * & \Gamma_{22} & 0 & 0\\ * & * & -I & 0\\ * & * & * & -I\end{bmatrix}\xi(t).$$

Now, let

$$\bar{\Theta} = \begin{bmatrix}\Theta_{11} & \Phi_{12} & P_iD_i & \Phi_{14} & 0\\ * & \Gamma_{22} & 0 & 0 & 0\\ * & * & -I & 0 & 0\\ * & * & * & -I & 0\\ * & * & * & * & 0\end{bmatrix},$$

$$\mathcal{S}^\top = \begin{bmatrix}-B_i^\top P_i + a_1V_i^\top B_i^\top & 0 & 0 & 0 & a_1V_i^\top\end{bmatrix},$$

and

$$H = \begin{bmatrix}(1-\overline{\kappa}_d)(1-\overline{\kappa}_c)K_iC_i & (1-\overline{\kappa}_d)(1-\overline{\kappa}_c)K_i & 0 & (1-\overline{\kappa}_d)\overline{\kappa}_cK_i & -I\end{bmatrix},$$

where

$$\Theta_{11} = He(P_i(A_i + (1-\overline{\kappa}_d)(1-\overline{\kappa}_c)B_iK_iC_i)) + \sum_{m=1}^{s_1}\pi_{im}P_m + \rho I - \alpha P_i + (1+\frac{1}{\theta})C_i^\top\widetilde{D}\widetilde{\Omega}C_i.$$

Then, it is easy to show that

$$\bar{\Theta} + He(\mathcal{S}H) = \begin{bmatrix}\Gamma_{11} & \Gamma_{12} & P_iD_i & \Gamma_{14} & \Gamma_{15}\\ * & \Gamma_{22} & 0 & 0 & \Gamma_{25}\\ * & * & -I & 0 & 0\\ * & * & * & -I & \Gamma_{45}\\ * & * & * & * & \Gamma_{55}\end{bmatrix}.$$

From (6), it is obvious that $\bar{\Theta} + He(\mathcal{S}H) < 0$. By employing Lemma 1, the above linear matrix inequality (LMI) is identical to $H^{\perp\top}\bar{\Theta}H^\perp < 0$, where

$$H^\perp = \begin{bmatrix}I & 0 & 0 & 0\\ 0 & I & 0 & 0\\ 0 & 0 & I & 0\\ 0 & 0 & 0 & I\\ (1-\overline{\kappa}_d)(1-\overline{\kappa}_c)K_iC_i & (1-\overline{\kappa}_d)(1-\overline{\kappa}_c)K_i & 0 & (1-\overline{\kappa}_d)\overline{\kappa}_cK_i\end{bmatrix}.$$

And we can calculate that $H^{\perp\top}\bar{\Theta}H^\perp = \Theta$, so $\Theta < 0$, in which

$$\Theta = \begin{bmatrix}\Theta_{11} & \Phi_{12} & P_iD_i & \Phi_{14}\\ * & \Gamma_{22} & 0 & 0\\ * & * & -I & 0\\ * & * & * & -I\end{bmatrix}.$$

Since $\Theta < 0$, it guarantees $J_1 < 0$, and then the following is ensured:

$$\mathcal{I}(V(x(t),r_t)) - \alpha V(x(t),r_t) - w^\top(t)w(t) < 0. \tag{11}$$

By multiplying both sides of (11) by $e^{-\alpha t}$ and integrating the result, which yields that

$$e^{-\alpha t}V(x(t),r_t) - V(x(0),r_0) < \int_0^t e^{-\alpha\tau}w^\top(\tau)w(\tau)d\tau.$$

By (7) and $x^\top(0)\mathcal{R}x(0) \le c_1$, it leads that $e^{-\alpha t}V(x(t),r_t) < \beta c_1 + \mathfrak{y}(0) + \int_0^t e^{-\alpha\tau}w^\top(\tau)w(\tau)d\tau$, for all $t \in [t_k, t_{k+1}) \subset [0,T]$. From (7) and (8), we obtain $x^\top(t)\mathcal{R}x(t) < c_2$ for all $t \in [t_k, t_{k+1}) \subset [0,T]$.

Now, the next step is to prove that the finite-time H_2-gain of the system (5) satisfies $J((5), E_0, T) < \gamma$. To make the notation more straightforward, we write $\|y(t)\|_{L_\infty,[0,T]}$ as $\|y(t)\|_\infty$ and $\|w(t)\|_{L_2,[0,T]}$ as $\|w(t)\|_2$, respectively. We define

$$J_3 := \mathcal{E}[\ \|y(t)\|_\infty^2 - \gamma^2\|w(t)\|_2^2 - \gamma^2 x^\top(0)E_0x(0)\ ].$$

Since $V(x(0),r_0) - V(x(T),r_T) + \mathcal{E}[\int_0^T \mathcal{I}(V(x(t),r_t))dt] = 0$, J_3 is rewritten as

$$\begin{aligned} J_3 = \mathcal{E}[\ \|y(t)\|_\infty^2 + \gamma^2 \int_0^T (-w^\top(t)w(t))\ dt - \gamma^2 x^\top(0)E_0x(0)\ ] + \gamma^2\mathcal{E}[\int_0^T \mathcal{I}(V(x(t),r_t))dt] - \gamma^2\mathfrak{y}(T) \\ - \gamma^2 x^\top(T)P_{r_T}x(T) + \gamma^2 x^\top(0)P_{r_0}x(0) + \gamma^2\mathfrak{y}(0). \end{aligned}$$

From (10) and letting Φ as follows

$$\Phi = \begin{bmatrix} \Phi_{11} & \Phi_{12} & P_iD_i & \Phi_{14} \\ * & \Gamma_{22} & 0 & 0 \\ * & * & -I & 0 \\ * & * & * & -I \end{bmatrix},$$

we get

$$J_3 < \|y(t)\|_\infty^2 + \gamma^2 \int_0^T \xi^\top(t)\Phi\xi(t)\ dt - \gamma^2 x^\top(T)P_{r_T}x(T) - \gamma^2\mathfrak{y}(T) + \gamma^2\mathfrak{y}(0) + \gamma^2 x^\top(0)(P_{r_0} - E_0)x(0).$$

According to $\|y(t)\|_\infty^2 = sup_{t\in[0,T]}(y^\top(t)y(t))$, it yields

$$\begin{aligned} J_3 < \ & sup_{t\in[0,T]}(x^\top(t)C_i^\top C_ix(t)) + \gamma^2 \int_0^T \xi^\top(t)\Phi\xi(t)\ dt - \gamma^2 x^\top(T)P_{r_t}x(T) - \gamma^2\mathfrak{y}(T) \\ & + \gamma^2 x^\top(0)(P_{r_0} - E_0 + \phi I)x(0). \end{aligned}$$

By hypotheses (9), $J_3 < 0$. Namely, $J((5), E_0, T) < \gamma$. Hence, Theorem 1 is proved. □

Remark 2. *Recall the internal dynamic function $\mathfrak{y}(t) > 0$ satisfies $\dot{\mathfrak{y}}(t) = -\lambda\mathfrak{y}(t) + y^\top(t_k)\widetilde{D}\widetilde{\Omega}y(t_k) - e^\top(t)\widetilde{\Omega}e(t)$. Then it becomes evident that $\mathfrak{y}(t) \le \mathfrak{y}(0)e^{-(\lambda+1)t}$. Thus, $\mathfrak{y}(t) \to 0$ as $t \to \infty$. Within $t \in [t_k, t_{k+1}) \subset [0,T]$, it is possible that there exists the scalar c_2 with $0 < c_1 < c_2$ satisfying $x^\top(t)\mathcal{R}x(t) + \mathfrak{y}(t) < c_2$ for all $t \in [t_k, t_{k+1})$, which implies $x^\top(t)\mathcal{R}x(t) < c_2$ for all $t \in [t_k, t_{k+1})$.*

Remark 3. *In the proof of Theorem 1, there are coupling terms $P_iB_iK_iC_i$ and $P_iB_iK_i$ in the block matrix Θ which cannot be solved by LMI toolbox in MATLAB. In order to overcome this, we introduce $K_i = V_i^{-1}W_i$, $P_iB_iK_iC_i = (P_iB_i - B_iV_i)K_iC_i + B_iW_iC_i$, and $P_iB_iK_i = (P_iB_i - B_iV_i)K_i + B_iW_i$. So, we can transform $\Theta < 0$ to a solvable form (6).*

3.2. Dynamic OFC design under the same dynamic ETS

From now on, simply write $\kappa_d(t)$ as κ_d and $\kappa_c(t)$ as κ_c, respectively. In this subsection, we design a mode-dependent dynamic OFC under the multiple cyber attacks.

$$\begin{aligned}\dot{x}_c(t) &= K_1(r_t)x_c(t) + K_2(r_t)y_a(t),\\ \mathfrak{u}(t) &= K_3(r_t)x_c(t) + K_4(r_t)y_a(t), \quad t \in [t_k, t_{k+1})\end{aligned} \tag{12}$$

where $x_c(t) \in \mathbb{R}^{n_x}$ is the controller state with $x_c(0) = 0$.
Combining the system (1) and (12) with $r_t = i$ and letting an augmented vector $\bar{x}(t) := [x^\top(t) \;\; x_c^\top(t)]^\top$ and $e(t) := y(t_k) - y(t)$, the attacked system is expressed as

$$\begin{cases}\dot{\bar{x}}(t) = \bar{A}_i\bar{x}(t) + \bar{B}_i e(t) + \bar{D}_i w(t) + \bar{E}_i g(t),\\ y(t) = \bar{C}_i\bar{x}(t), \quad t \in [t_k, t_{k+1}) \subset [0, T],\end{cases} \tag{13}$$

where

$$\bar{A}_i = \begin{bmatrix} A_i + (1-\kappa_d)(1-\kappa_c)B_iK_{4i}C_i & B_iK_{3i} \\ (1-\kappa_d)(1-\kappa_c)K_{2i}C_i & K_{1i}\end{bmatrix}, \quad \bar{B}_i = \begin{bmatrix}(1-\kappa_d)(1-\kappa_c)B_iK_{4i}\\ (1-\kappa_d)(1-\kappa_c)K_{2i}\end{bmatrix}, \tag{14}$$

$$\bar{D}_i = \begin{bmatrix} D_i \\ 0\end{bmatrix}, \quad \bar{E}_i = \begin{bmatrix}(1-\kappa_d)\kappa_c B_iK_{4i}\\ (1-\kappa_d)\kappa_c K_{2i}\end{bmatrix}, \quad \bar{C}_i = \begin{bmatrix} C_i & 0\end{bmatrix}. \tag{15}$$

By employing the dynamic OFC under the same dynamic ETS and the multiple cyber attacks, Theorem 2 provides sufficient conditions to ensure that the augmented system (13) is stochastically FTB with finite-time H_2-gain performance index γ.

Theorem 2. *Let $\alpha > 0, d > 0, T > 0, \lambda > 0, a_1 > 0$, $\rho > 0$, $c_1 > 0$ and $\lambda > \frac{1}{\theta}$. Suppose that Assumptions 1 - 4 hold, and the initial condition of the internal dynamic function $\mathfrak{y}(t)$ satisfies $\mathfrak{y}(0) = \phi\bar{x}^\top(0)\bar{x}(0)$ for a scalar $\phi > 0$. If there exist $\bar{P}_i := diag\{P_{1i}, P_{2i}\}$ with $P_{1i}^\top = P_{1i} > 0$ and $P_{2i}^\top = P_{2i} > 0$, $\widetilde{\Omega}^\top = \widetilde{\Omega} > 0$, matrices M_i, N_i, V_i, W_{1i}, W_{2i} for all $i \in S_1$, and scalars $\beta > 1$, $\gamma > 0$, $c_2 > 0$ with $c_1 < c_2$ such that*

$$\begin{bmatrix}\Lambda_{11} & \Lambda_{12} & \Lambda_{13} & P_{1i}D_i & \Lambda_{15} & \Lambda_{16}\\ * & \Lambda_{22} & \Lambda_{23} & 0 & \Lambda_{25} & a_1W_{2i}^\top\\ * & * & \Omega_{33} & 0 & 0 & \Lambda_{36}\\ * & * & * & -I & 0 & 0\\ * & * & * & * & -I & \Lambda_{56}\\ * & * & * & * & * & \Lambda_{66}\end{bmatrix} < 0, \tag{16}$$

$$\overline{\mathcal{R}} < \bar{P}_i < \beta\overline{\mathcal{R}}, \tag{17}$$

$$e^{\alpha T}(\beta c_1 + d + \mathfrak{y}(0)) < c_2, \tag{18}$$

$$\frac{1}{\gamma^2}\bar{C}_i^\top\bar{C}_i \le \bar{P}_i \le \overline{E}_0 - \phi I, \tag{19}$$

for all $t \in [t_k, t_{k+1}) \subset [0, T]$, where

$$\Lambda_{11} = He(P_{1i}A_i + a_1(1-\overline{\kappa}_d)(1-\overline{\kappa}_c)B_iW_{1i}C_i) + \rho I + \sum_{m=1}^{s_1}\pi_{im}P_{1m} - \alpha P_{1i} + (1+\frac{1}{\theta})C_i^\top\widetilde{D}\widetilde{\Omega}C_i,$$

$$\Lambda_{12} = a_1B_iW_{2i} + (1-\overline{\kappa}_d)(1-\overline{\kappa}_c)C_i^\top N_i^\top, \qquad \Lambda_{13} = a_1(1-\overline{\kappa}_d)(1-\overline{\kappa}_c)B_iW_{1i} + (1+\frac{1}{\theta})C_i^\top\widetilde{D}\widetilde{\Omega},$$

$$\Lambda_{15} = a_1(1-\overline{\kappa}_d)\overline{\kappa}_cB_iW_{1i}, \qquad \Lambda_{16} = P_{1i}B_i - a_1B_iV_i + a_1(1-\overline{\kappa}_d)(1-\overline{\kappa}_c)C_i^\top W_{1i}^\top,$$

$$\Lambda_{22} = He(M_i) + \sum_{m=1}^{s_1}\pi_{im}P_{2m} - \alpha P_{2i}, \qquad \Lambda_{23} = (1-\overline{\kappa}_d)(1-\overline{\kappa}_c)N_i,$$

$$\Lambda_{25} = (1-\overline{\kappa}_d)\overline{\kappa}_cN_i, \qquad \Omega_{33} = -(1+\frac{1}{\theta})(I-\widetilde{D})\widetilde{\Omega},$$

$$\Lambda_{36} = a_1(1-\overline{\kappa}_d)(1-\overline{\kappa}_c)W_{1i}^\top, \qquad \Lambda_{56} = a_1(1-\overline{\kappa}_d)\overline{\kappa}_cW_{1i}^\top, \qquad \Lambda_{66} = -a_1He(V_i),$$

and $\overline{\mathcal{R}}$ *and* $\overline{E}_0$ *are given matrices with* $\overline{\mathcal{R}}^\top = \overline{\mathcal{R}} > 0$ *and* $\overline{E}_0^\top = \overline{E}_0 > 0$*, then the enlarged closed-loop system (13) is stochastically FTB and meet the finite-time* H_2*-gain performance index* γ*. In this instance,* $K_{1i} = P_{2i}^{-1}M_i$*,* $K_{2i} = P_{2i}^{-1}N_i$*,* $K_{4i} = V_i^{-1}W_{1i}$ *and* $K_{3i} = V_i^{-1}W_{2i}$*.*

Proof. For each fixed $i \in S_1$, we construct

$$V(\bar{x}(t), i) = \bar{x}^\top(t)\bar{P}_i\bar{x}(t) + \mathfrak{y}(t),$$

where $\bar{P}_i := \text{diag}\{P_{1i}, P_{2i}\}$ with $P_{1i}^\top = P_{1i} > 0$ and $P_{2i}^\top = P_{2i} > 0$.
Through the application of $\mathcal{I}$, this leads to

$$\begin{aligned}
\mathcal{E}[\mathcal{I}(V(\bar{x}(t), i))] &= \mathcal{E}[\dot{\bar{x}}^\top(t)\bar{P}_i\bar{x}(t) + \bar{x}^\top(t)\bar{P}_i\dot{\bar{x}}(t) + \bar{x}^\top(t)(\sum_{m=1}^{s_1}\pi_{im}\bar{P}_m)\bar{x}(t) + \dot{\mathfrak{y}}(t)] \\
&= \bar{x}^\top(t)\bar{A}_i^\top(t)\bar{P}_i\bar{x}(t) + e^\top(t)\bar{B}_i^\top\bar{P}_i\bar{x}(t) + \bar{x}^\top(t)\bar{P}_i\bar{A}_i\bar{x}(t) + \bar{x}^\top(t)\bar{P}_i\bar{B}_ie(t) \\
&\quad + w^\top(t)\bar{D}_i^\top\bar{P}_i\bar{x}(t) + \bar{x}^\top(t)\bar{P}_i\bar{D}_iw(t) + \bar{x}^\top(t)(\sum_{m=1}^{s_1}\pi_{im}\bar{P}_m)\bar{x}(t) \\
&\quad + \bar{x}^\top(t)\bar{P}_i\bar{E}_ig(t) + g^\top(t)\bar{E}_i^\top\bar{P}_i\bar{x}(t) - \lambda\mathfrak{y}(t) + y^\top(t_k)\widetilde{D}\widetilde{\Omega}y(t_k) - e^\top(t)\widetilde{\Omega}e(t).
\end{aligned}$$

By the same event-triggering condition, the above equation becomes

$$\begin{aligned}
\mathcal{E}[\mathcal{I}(V(\bar{x}(t), i))] \leq& \bar{x}^\top(t)\{He(\bar{P}_i\bar{A}_i) + \sum_{m=1}^{s_1}\pi_{im}\bar{P}_m\}\bar{x}(t) + \bar{x}^\top(t)\bar{P}_i\bar{B}_ie(t) + e^\top(t)\bar{B}_i^\top\bar{P}_i\bar{x}(t) \\
&+ \bar{x}^\top(t)\bar{P}_i\bar{D}_iw(t) + w^\top(t)\bar{D}_i^\top\bar{P}_i\bar{x}(t) + \bar{x}^\top(t)\bar{P}_i\bar{E}_ig(t) + g^\top(t)\bar{E}_i^\top\bar{P}_i\bar{x}(t) \\
&+ (\frac{1}{\theta} - \lambda)\mathfrak{y}(t) + (1 + \frac{1}{\theta})y^\top(t_k)\widetilde{D}\widetilde{\Omega}y(t_k) - (1 + \frac{1}{\theta})e^\top(t)\widetilde{\Omega}e(t).
\end{aligned}$$

From $(\frac{1}{\theta} - \lambda)\mathfrak{y}(t) < 0$ and Assumption 4, we get

$$\begin{aligned}
\mathcal{E}[\mathcal{I}(V(\bar{x}(t), i))] <& \bar{x}^\top(t)\{He(\bar{P}_i\bar{A}_i) + \sum_{m=1}^{s_1}\pi_{im}\bar{P}_m + (1 + \frac{1}{\theta})\bar{C}_i^\top\widetilde{D}\widetilde{\Omega}\bar{C}_i\}\bar{x}(t) + \rho x^\top(t)x(t) \\
&+ \bar{x}^\top(t)(\bar{P}_i\bar{B}_i + (1 + \frac{1}{\theta})\bar{C}_i^\top\widetilde{D}\widetilde{\Omega})e(t) + e^\top(t)(\bar{B}_i^\top\bar{P}_i + (1 + \frac{1}{\theta})\widetilde{D}\widetilde{\Omega}\bar{C}_i)\bar{x}(t) \\
&+ \bar{x}^\top(t)\bar{P}_i\bar{D}_iw(t) + w^\top(t)\bar{D}_i^\top\bar{P}_i\bar{x}(t) + \bar{x}^\top(t)\bar{P}_i\bar{E}_ig(t) + g^\top(t)\bar{E}_i^\top\bar{P}_i\bar{x}(t) \\
&- (1 + \frac{1}{\theta})e^\top(t)(I - \widetilde{D})\widetilde{\Omega}e(t) - g^\top(t)g(t).
\end{aligned}$$

Calculating specifically by applying matrices (14) and (15), the above inequality yields

$$\begin{aligned}
\mathcal{E}[\mathcal{I}(V(\bar{x}(t),i))] < x^\top(t)\{He(P_{1i}(A_i+(1-\overline{\kappa}_d)(1-\overline{\kappa}_c)B_iK_{4i}C_i)) + \sum_{m=1}^{s_1}\pi_{im}P_{1m} + \rho I \\
+ (1+\frac{1}{\theta})C_i^\top\widetilde{D}\widetilde{\Omega}C_i\}x(t) + x^\top(t)(P_{1i}B_iK_{3i} + (1-\overline{\kappa}_d)(1-\overline{\kappa}_c)C_i^\top K_{2i}^\top P_{2i})x_c(t) \\
+ x_c^\top(t)((1-\overline{\kappa}_d)(1-\overline{\kappa}_c)P_{2i}K_{2i}C_i + K_{3i}^\top B_i^\top P_{1i})x(t) + x_c^\top(t)\{He(P_{2i}K_{1i}) + \sum_{m=1}^{s_1}\pi_{im}P_{2m}\}x_c(t) \\
+ x^\top(t)((1-\overline{\kappa}_d)(1-\overline{\kappa}_c)P_{1i}B_iK_{4i} + (1+\frac{1}{\theta})C_i^\top\widetilde{D}\widetilde{\Omega})e(t) \\
+ (1-\overline{\kappa}_d)(1-\overline{\kappa}_c)x_c^\top(t)P_{2i}K_{2i}e(t) + (1-\overline{\kappa}_d)(1-\overline{\kappa}_c)e^\top(t)K_{2i}^\top P_{2i}x_c(t) \\
+ e^\top(t)((1-\overline{\kappa}_d)(1-\overline{\kappa}_c)K_{4i}^\top B_i^\top P_{1i} + (1+\frac{1}{\theta})\widetilde{D}\widetilde{\Omega}C_i)x(t) + (1-\overline{\kappa}_d)\overline{\kappa}_c x^\top(t)P_{1i}B_iK_{4i}g(t) \\
+ (1-\overline{\kappa}_d)\overline{\kappa}_c g^\top(t)K_{4i}^\top B_i^\top P_{1i}x(t) + (1-\overline{\kappa}_d)\overline{\kappa}_c x_c^\top(t)P_{2i}K_{2i}g(t) + (1-\overline{\kappa}_d)\overline{\kappa}_c g^\top(t)K_{2i}^\top P_{2i}x_c(t) \\
+ x^\top(t)P_{1i}D_iw(t) + w^\top(t)D_i^\top P_{1i}x(t) - (1+\frac{1}{\theta})e^\top(t)(I-\widetilde{D})\widetilde{\Omega}e(t) - g^\top(t)g(t). \qquad (20)
\end{aligned}$$

Let $\mu^\top(t) := [x^\top(t) \;\; x_c^\top(t) \;\; e^\top(t) \;\; w^\top(t) \;\; g^\top(t)]$. The above inequality (20) becomes

$$\mathcal{E}[\mathcal{I}(V(\bar{x}(t),i))] < \mu^\top(t)\begin{bmatrix}\Omega_{11} & \Omega_{12} & \Omega_{13} & P_{1i}D_i & \Omega_{15}\\ * & \Omega_{22} & \Omega_{23} & 0 & \Omega_{25}\\ * & * & \Omega_{33} & 0 & 0\\ * & * & * & 0 & 0\\ * & * & * & * & -I\end{bmatrix}\mu(t), \qquad (21)$$

where $\Omega_{11} = He(P_{1i}(A_i+(1-\overline{\kappa}_d)(1-\overline{\kappa}_c)B_iK_{4i}C_i))+\sum_{m=1}^{s_1}\pi_{im}P_{1m}+\rho I+(1+\frac{1}{\theta})C_i^\top\widetilde{D}\widetilde{\Omega}C_i$, $\Omega_{12} = P_{1i}B_iK_{3i}+(1-\overline{\kappa}_d)(1-\overline{\kappa}_c)C_i^\top K_{2i}^\top P_{2i}$, $\Omega_{13} = (1-\overline{\kappa}_d)(1-\overline{\kappa}_c)P_{1i}B_iK_{4i} + (1+\frac{1}{\theta})C_i^\top\widetilde{D}\widetilde{\Omega}$, $\Omega_{15} = (1-\overline{\kappa}_d)\overline{\kappa}_cP_{1i}B_iK_{4i}$, $\Omega_{22} = He(P_{2i}K_{1i}) + \sum_{m=1}^{s_1}\pi_{im}P_{2m}$, $\Omega_{23} = (1-\overline{\kappa}_d)(1-\overline{\kappa}_c)P_{2i}K_{2i}$, $\Omega_{25} = (1-\overline{\kappa}_d)\overline{\kappa}_cP_{2i}K_{2i}$, and $\Omega_{33} = -(1+\frac{1}{\theta})(I-\widetilde{D})\widetilde{\Omega}$.

Defining $J_2 := \mathcal{E}[\mathcal{I}(V(\bar{x}(t),i)) - \alpha V(\bar{x}(t),i) - w^\top(t)w(t)]$. Since $\alpha > 0, \mathfrak{y}(t) > 0$ for all $t \in [t_k, t_{k+1}) \subset [0,T]$ and based on (21), J_2 yields

$$J_2 \;<\; \mu^\top(t)\begin{bmatrix}\Omega_{11}-\alpha P_{1i} & \Omega_{12} & \Omega_{13} & P_{1i}D_i & \Omega_{15}\\ * & \Omega_{22}-\alpha P_{2i} & \Omega_{23} & 0 & \Omega_{25}\\ * & * & \Omega_{33} & 0 & 0\\ * & * & * & -I & 0\\ * & * & * & * & -I\end{bmatrix}\mu(t). \qquad (22)$$

Now, letting

$$\bar{\Omega} = \begin{bmatrix}\Omega'_{11} & \Omega_{12} & \Omega_{13} & P_{1i}D_i & \Omega_{15} & 0\\ * & \Omega'_{22} & \Omega_{23} & 0 & \Omega_{25} & 0\\ * & * & \Omega_{33} & 0 & 0 & 0\\ * & * & * & -I & 0 & 0\\ * & * & * & * & -I & 0\\ * & * & * & * & * & 0\end{bmatrix},$$

$$\mathcal{S}^\top = \begin{bmatrix}-B_i^\top P_{1i} + a_1V_i^\top B_i^\top & 0 & 0 & 0 & 0 & a_1V_i^\top\end{bmatrix},$$

and

$$H = \begin{bmatrix}h_{51} & K_{3i} & h_{53} & 0 & h_{55} & -I\end{bmatrix},$$

where $\Omega'_{11} = \Omega_{11} - \alpha P_{1i}$, $\Omega'_{22} = \Omega_{22} - \alpha P_{2i}$, $h_{51} = (1-\overline{\kappa}_d)(1-\overline{\kappa}_c)K_{4i}C_i$, $h_{53} = (1-\overline{\kappa}_d)(1-\overline{\kappa}_c)K_{4i}$ and $h_{55} = (1-\overline{\kappa}_d)\overline{\kappa}_c K_{4i}$, it is easy to show that

$$\bar{\Omega} + He(\mathcal{S}H) = \begin{bmatrix} \Lambda_{11} & \Lambda_{12} & \Lambda_{13} & P_{1i}D_i & \Lambda_{15} & \Lambda_{16} \\ * & \Lambda_{22} & \Lambda_{23} & 0 & \Lambda_{25} & a_1 W_{2i}^\top \\ * & * & \Omega_{33} & 0 & 0 & \Lambda_{36} \\ * & * & * & -I & 0 & 0 \\ * & * & * & * & -I & \Lambda_{56} \\ * & * & * & * & * & \Lambda_{66} \end{bmatrix}.$$

By the hypothesis (16), it is obvious that $\bar{\Omega} + He(\mathcal{S}H) < 0$. According to Lemma 1, the above LMI is equivalent to $H^{\perp\top}\bar{\Omega}H^{\perp} < 0$, where

$$H^{\perp} = \begin{bmatrix} I & 0 & 0 & 0 & 0 & 0 \\ 0 & I & 0 & 0 & 0 & 0 \\ 0 & 0 & I & 0 & 0 & 0 \\ 0 & 0 & 0 & I & 0 & 0 \\ 0 & 0 & 0 & 0 & I & 0 \\ 0 & 0 & 0 & 0 & 0 & I \\ h_{51} & K_{3i} & h_{53} & 0 & h_{55} & 0 \end{bmatrix}.$$

And we can find $H^{\perp\top}\bar{\Omega}H^{\perp} = \Omega$, so $\Omega < 0$, in which

$$\Omega = \begin{bmatrix} \Omega'_{11} & \Omega_{12} & \Omega_{13} & P_{1i}D_i & \Omega_{15} \\ * & \Omega'_{22} & \Omega_{23} & 0 & \Omega_{25} \\ * & * & \Omega_{33} & 0 & 0 \\ * & * & * & -I & 0 \\ * & * & * & * & -I \end{bmatrix}.$$

It guarantees $J_2 < 0$. The rest of this proof follows similarly to the latter portion of Theorem 1, therefore ensuring that the system (13) is stochastically FTB with respect to $(c_1, c_2, \overline{\mathcal{R}}, T, d)$ and the finite-time H_2-gain satisfies $J((13), \overline{E}_0, T) < \gamma$. □

Remark 4. *In the process of proving Theorem 2, the block matrix Ω contains coupling terms $P_{1i}B_iK_{4i}C_i$, $P_{1i}B_iK_{3i}$ and $P_{1i}B_iK_{4i}$ that cannot be resolved using MATLAB's LMI toolbox. To address this, we introduce $K_{4i} = V_i^{-1}W_{1i}$, $K_{3i} = V_i^{-1}W_{2i}$ and $P_{1i}B_iK_{4i}C_i = (P_{1i}B_i - B_iV_i)K_{4i}C_i + B_iW_{1i}C_i$, enabling us to reformulate $\Omega < 0$ into a solvable form (16).*

4. Example

In this part, we shall simulate borrowing a model of F-404 aircraft engine from the work of [33]. The aircraft engine model can be represented by the system (1) featuring four modes of operation such that:

$$A_1 = \begin{bmatrix} -1.46 & 0 & 2.428 \\ 0.1643 - 0.5*5 & 0.4-5 & -0.3788 \\ 0.3107 & 0 & -2.23 \end{bmatrix}, \quad A_2 = \begin{bmatrix} -1.46 & 0 & 2.428 \\ 0.1643 - 0.5*6 & 0.4-6 & -0.3788 \\ 0.3107 & 0 & -2.23 \end{bmatrix},$$

$$A_3 = \begin{bmatrix} -1.46 & 0 & 2.428 \\ 0.1643 - 0.5*7 & 0.4-7 & -0.3788 \\ 0.3107 & 0 & -2.23 \end{bmatrix}, \quad A_4 = \begin{bmatrix} -1.46 & 0 & 2.428 \\ 0.1643 - 0.5*8 & 0.4-8 & -0.3788 \\ 0.3107 & 0 & -2.23 \end{bmatrix},$$

$$B_i = \begin{bmatrix} 0 \\ 0 \\ 1 \end{bmatrix}, C_i = \begin{bmatrix} 1 & 1 & 0 \\ 0 & 0 & 1 \end{bmatrix}, D_i = \begin{bmatrix} 0.2 \\ 0.2 \\ 0.0 \end{bmatrix},$$

for all $i \in \{1, 2, 3, 4\}$. It is assumed $x(0) = [-1\ 0.5\ 0.8]^\top$ and the TRM is

$$\Pi = \begin{bmatrix} -2.4 & 2.2 & 0.1 & 0.1 \\ 0.1 & -1.9 & 1.7 & 0.1 \\ 1.2 & 0.3 & -1.8 & 0.3 \\ 2.6 & 0.1 & 0.1 & -2.8 \end{bmatrix}.$$

The other parameters set as $\alpha = 0.9$, $d = 0.5$, $\lambda = 0.9$, $a_1 = 1.2, c_1 = 0.3$, $\phi = 0.1, \rho = 0.6$, $\mathcal{R} = 0.1I$, $E_0 = I$, $\overline{\kappa}_d = 0.2, \overline{\kappa}_c = 0.3$, and $w(t) = 0.05 \sin t$.

4.1. Example 1

First, to validate the effectiveness of the proposed ETS (2), it is compared with the existing ETSs in [11] and [12]. The triggering parameters for the two existing results and the proposed ETS are listed as follows:

Table 1: Parameters for different ETSs

Methods	Parameters
Theorem 1	$\widetilde{D} = diag\{0.01, 0.31\}$, $\theta = 1.2$
Theorem 2	$\widetilde{D} = diag\{0.01, 0.31\}$, $\theta = 1.2$
[11]	$\widetilde{D} = 0.01$
[12]	$\widetilde{D} = diag\{0.01, 0.01\}$, $\theta = 1.2$

Then, the simulation curves are displayed in Figs. 2-4, and the number of triggering times are provided in Table 2.

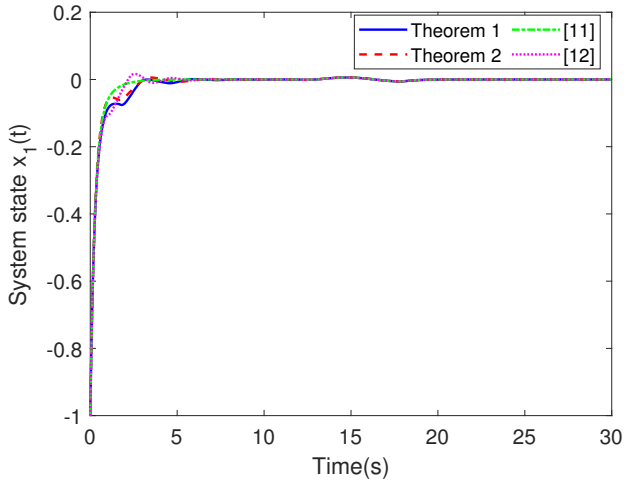

Figure 2: $x_1(t)$ under different methods

Table 2: The number of triggering times $N(T)$ and the ratio $N(T)/T$

Methods	Theorem 2	Theorem 1	[12]	[11]
$N(T)$	77	79	91	451
Ratio	2.56	2.63	3.03	15.03

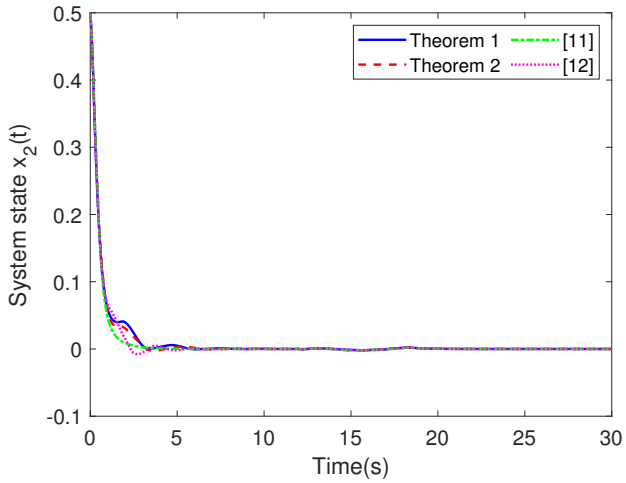

Figure 3: $x_2(t)$ under different methods

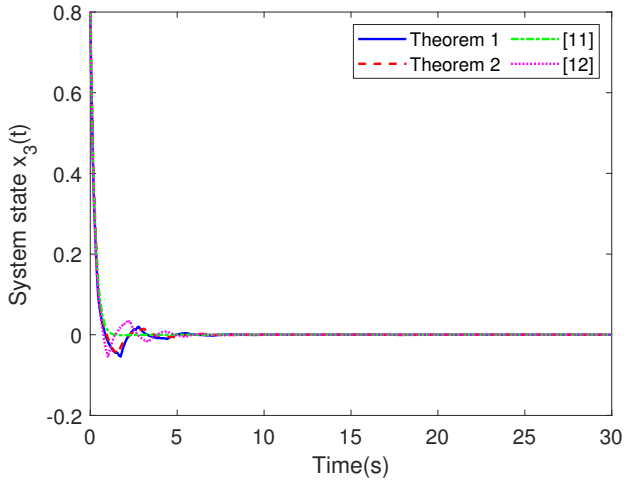

Figure 4: $x_3(t)$ under different methods

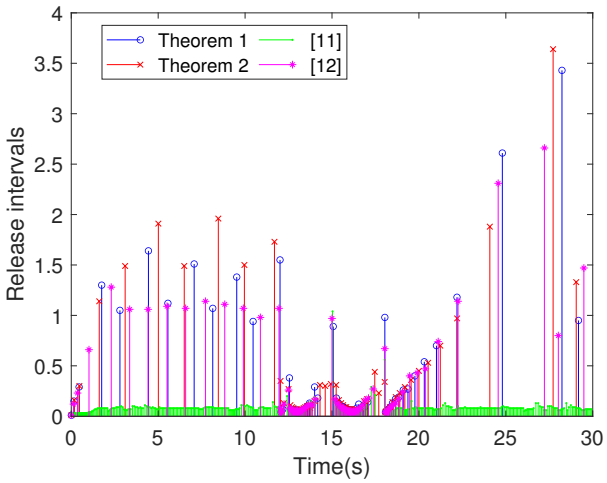

Figure 5: Release intervals under different methods

From the system state curves in Figs. 2-4, the performance of the proposed method is almost the same as that of the system under the two compared methods. As can be seen from Fig. 5, the proposed ETS is able to produce larger triggering intervals compared to existing results [11] and [12].

To quantify the communication efficiency, we use a ratio $\frac{N(T)}{T}$ as a communication metrics, where T is the simulation time and $N(T)$ is the number of triggering times in the interval $[0, T]$. All simulations were conducted over the same simulation time $T = 30$. As shown in Table 2, the ratio of the proposed method is less than 3, whereas the ratios corresponding to the existing results in [12] and [11] are 3.03 and 15.03, respectively. This indicates that the proposed method is more efficient, as a smaller ratio reflects fewer the number of triggering times over the same simulation time. We can also see that the ratio of 2.56 obtained by the dynamic OFC (Theorem 2) is slightly smaller than the 2.63 by the static OFC (Theorem 1). Therefore, the general dynamic ETS proposed in Theorems 1 and 2 is more effective than the existing methods [11] and [12], and it can also be seen that the dynamic OFC method is slightly more effective than the static OFC under the same general ETS framework.

4.2. Example 2

Second, a simulation under attack parameters is presented. In order to fully demonstrate the impact of the cyber attacks, ETS is excluded. The attack parameters for three cases are listed as follows:

Table 3: Parameters for three cases

Case	Parameters
Case 1	$\overline{\kappa}_d = 0.9,\ \overline{\kappa}_c = 0.0$
Case 2	$\overline{\kappa}_d = 0.0,\ \overline{\kappa}_c = 0.9$
Case 3	$\overline{\kappa}_d = 0.0,\ \overline{\kappa}_c = 0.0$

Applying the above parameters, simulation curves are displayed in Figs. 6-8.

From Figs. 6-8, Case 1 (DoS attacks only) exhibits a longer convergence time than Case 3 (no attacks). Case 2 (deception attacks only) makes the controller calculate the control signal that includes the deception attack signal, which makes the system overshoot larger. Overall, the proposed method ensures the stability of the system under cyber attacks.

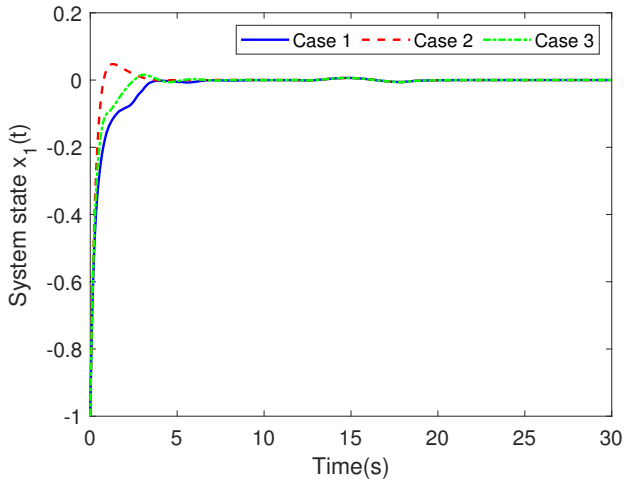

Figure 6: $x_1(t)$ under three cases

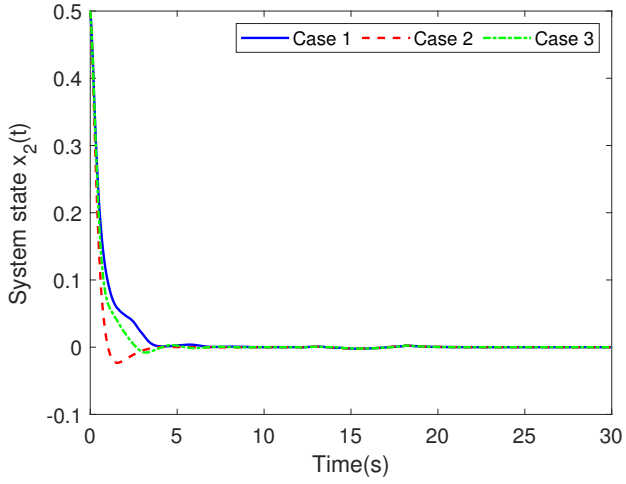

Figure 7: $x_2(t)$ under three cases

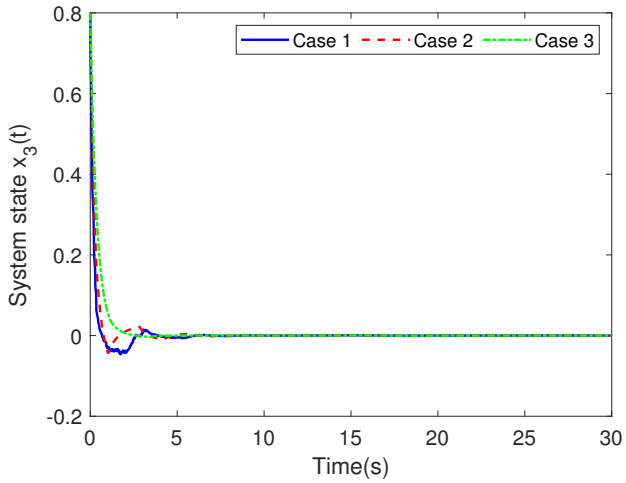

Figure 8: $x_3(t)$ under three cases

4.3. Example 3

Third, to demonstrate the event-triggering effects of the proposed general dynamic ETS (2), four cases are considered in Table 4 to examine the impact of the ET parameters on system performance. In all cases, the parameters λ and θ are chosen to satisfy constraint $\lambda > \frac{1}{\theta}$ in Theorem 1 and Theorem 2.

Table 4: Parameters for four cases

Case	Parameters
Case A	$\widetilde{D} = diag\{0.01, 0.01\}$, $\theta = 1.2$, $\lambda = 0.9$
Case B	$\widetilde{D} = diag\{0.1, 0.1\}$, $\theta = 1.2$, $\lambda = 0.9$
Case C	$\widetilde{D} = diag\{0.01, 0.01\}$, $\theta = 12$, $\lambda = 0.9$
Case D	$\widetilde{D} = diag\{0.01, 0.01\}$, $\theta = 1.2$, $\lambda = 9$

Table 5: The number of triggering times $N(T)$ for four cases

Case	A	B	C	D
$N(T)$	91	47	86	417

As shown in Figure 9-11 and Table 5, Case B has the fewest number of triggering times, and Case D has the least chattering. These results show the influence of ET parameters on system performance. Therefore, in practical applications, selecting appropriate ET parameters should balance triggering efficiency and overall system performance.

5. Conclusion

The dynamic event-triggered H_2 static and dynamic output-feedback secure finite-time control for networked MJSs subject to multiple cyber attacks has been discussed in this paper. A model for multiple cyber attacks has been used by introducing Bernoulli-distributed stochastic variables to characterize these attacks. To reduce communication resource usage, a general dynamic ETS has been implemented where the triggering threshold is in the form of a diagonal matrix. Mode-dependent static/dynamic output-feedback

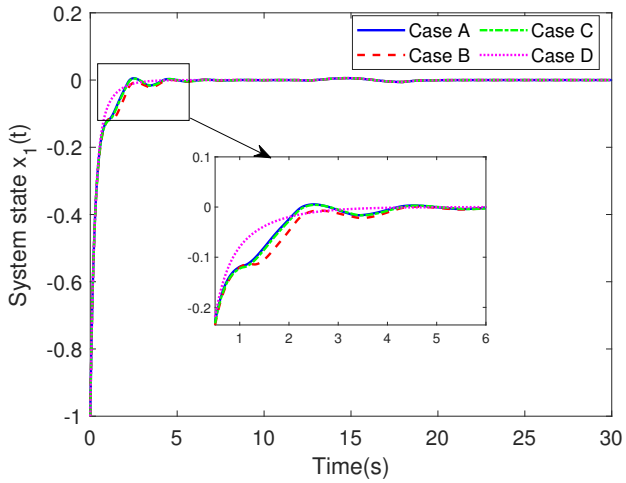

Figure 9: $x_1(t)$ under four cases

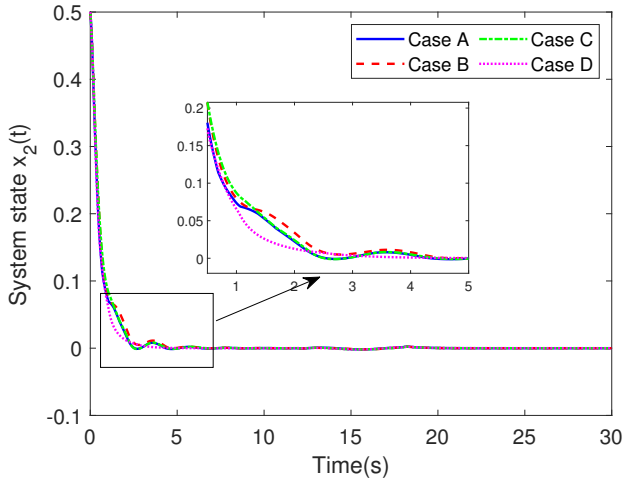

Figure 10: $x_2(t)$ under four cases

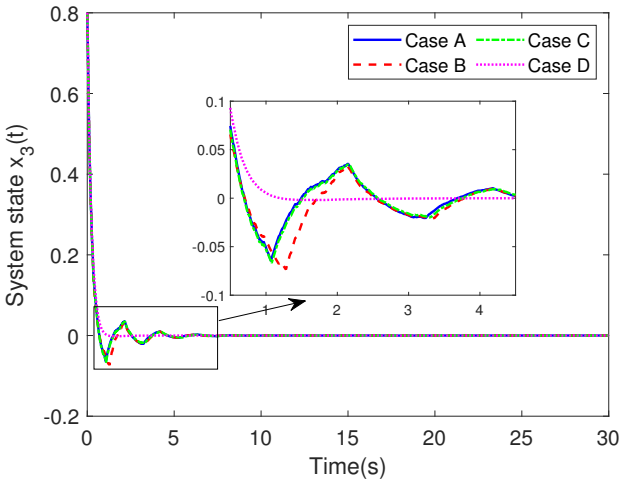

Figure 11: $x_3(t)$ under four cases

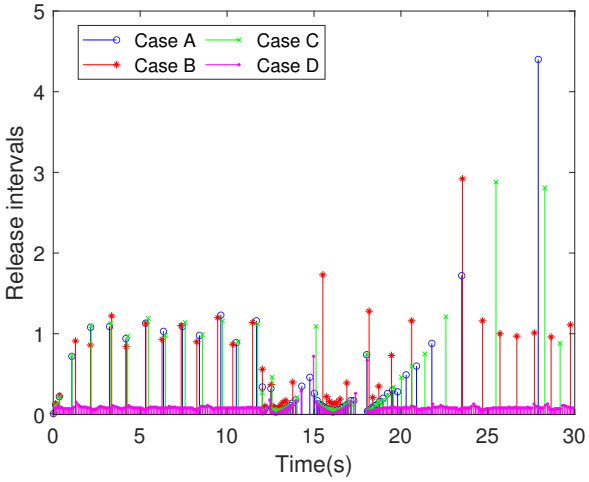

Figure 12: Release intervals

control schemes have been proposed to guarantee the FTB of the closed-loop system with finite-time H_2-gain performance. Finally, a comparative result has been supplied to confirm the validity of the suggested approach.

6. Acknowledgments

This work was supported by the National Research Foundation of Korea (NRF) grant funded by the Korea government(MSIT) (No. RS-2019-NR040065).

References

[1] S. Han, S. Park, S. Lee. Sampled-data-based iterative cost-learning model predictive control for T–S fuzzy systems. *IEEE Transactions on Systems, Man, and Cybernetics: Systems*, vol. 54, pp. 4701-4712, 2024.

[2] M. Kchaou, M. M. Tajudeen, M. S. Ali, G. Rajchakit, G. Shanthi, J. Cao. Asynchronous H_∞ control for IT2 fuzzy networked system subject to hybrid attacks via improved event-triggered scheme. *Information Sciences*, vol. 666, 120390, 2024.

[3] R.-C. Roman, R.-E. Precup, S. Preitl, A.-I. S.-Stinean, C.-A. B.-Dragos, E.-L.-Hedrea, E. M. Petriu. PI controller tuning via data-driven algorithms for shape memory alloy systems. *IFAC-PapersOnLine*, vol. 55, pp. 181-186, 2022.

[4] D. He, H. Wang, Y. Tian, R.-E. Precup, Model-free global sliding mode control using adaptive fuzzy system under constrained input amplitude and rate for mechatronic systems subject to mismatched disturbances. *Information Sciences*, vol. 697, 121769, 2025.

[5] R.-C. Roman, R.-E. Precup, E. M. Petriu, A.-I. Borlea. Hybrid data-driven active disturbance rejection sliding mode control with tower crane systems validation. *Romanian Journal of Information Science and Technology*, vol. 27, pp. 50-64, 2024.

[6] Y. Weng, M. Tian, N. Wang. Finite-time model-free adaptive control for MIMO nonlinear systems With adjustable fast convergence domain: theory and experiment. *IEEE Transactions on Industrial Electronics*, DOI: 10.1109/TIE.2025.3536547, 2025.

[7] A. Hentout, A. Maoudj, A. Kouider. Shortest path planning and efficient fuzzy logic control of mobile robots in indoor static and dynamic environments. *Romanian Journal of Information Science and Technology*, vol. 27, pp. 21-36, 2024.

[8] Y. Xia, K. Xiao, J. Cao, R.-E. Precup, Y. Arya, H.-K. Lam, L. Rutkowski. Stochastic neural network control for stochastic nonlinear systems with quadratic local asymmetric prescribed performance. *IEEE Transactions on Cybernetics*, vol. 55, pp. 867–879, 2025.

[9] J. Zhao, C. Yang, W. Gao. Reinforcement learning based optimal control of linear singularly perturbed systems. *IEEE Transactions on Circuits and Systems II: Express Briefs*, vol. 69, pp. 1362-1366, 2022.

[10] Y. Feng, M. Wu, L. Chen, X. Chen, W. Cao, S. Du, W. Pedrycz. Hybrid intelligent control based on condition identification for combustion process in heating furnace of compact strip production. *IEEE Transactions on Industrial Electronics*, vol. 69, pp. 2790–2800, 2022.

[11] C. Peng, T. C. Yang. Event-triggered communication and H_∞ control co-design for networked control systems. *Automatica*, vol. 49, no. 5, pp. 1326-1332, 2013.

[12] A. Girard. Dynamic triggering mechanisms for event-triggered control. *IEEE Transactions on Automatic Control*, vol. 60, no. 7, pp. 1992-1997, 2014.

[13] M. Shen, Y. Gu, J. H. Park, Y. Yi, W.-W. Che. Composite control of linear systems with event-triggered inputs and outputs. *IEEE Transactions on Circuits and Systems II: Express Briefs*, vol. 69, pp. 1154-1158, 2022.

[14] X. Chu, Z. Liu, L. Mao, X. Jin, Z. Peng, G. Wen. Robust event triggered control for lateral dynamics of intelligent vehicle with designable inter-event times. *IEEE Transactions on Circuits and Systems II: Express Briefs*, vol. 69, pp. 4349-4353, 2022.

[15] J. Tao, Z. Xiao, J. Chen, M. Lin, R. Lu, P. Shi, X. Wang. Event-triggered control for Markov jump systems subject to mismatched modes and strict dissipativity. *IEEE Transactions on Cybernetics*, vol. 53, pp. 1537-1546, 2023.

[16] X. Liu, X. Su, P. Shi, C. Shen, Y. Peng. Event-triggered sliding mode control of nonlinear dynamic systems, *Automatica*, vol. 112, 108738, 2020.

[17] T. Shi, P. Shi, Z.-G. Wu. Finite-time stochastic dissipative output tracking control of semi-Markov jump systems via an adaptive event-triggered mechanism. *International Journal of Robust and Nonlinear Control*, vol. 33, pp. 7774-7792, 2023.

[18] J. Liu, Z.-G. Wu, D. Yue, J. H. Park. Stabilization of networked control systems with hybrid-driven mechanism and probabilistic cyber attacks. *IEEE Transactions on Systems, Man, and Cybernetics: Systems*, vol. 51, pp. 943–953, 2021.

[19] H. Sun, C. Peng, Y. Wang, Y.-C. Tian. Output-based resilient event-triggered control for networked control systems under denial of service attacks. *IET Control Theory & Applications*, vol. 13, pp. 2521-2528, 2019.

[20] M. Rouamel, L.A.L. Oliveira, F. Bourahala, K. Guelton, K.M.D. Motchon. Networked control systems design under deception attacks with dynamic event-triggering mechanism. *IEEE Control Systems Letters*, vol. 7, pp. 3265-3270, 2023.

[21] S. Hu, D. Yue, Q-L. Han, X. Xie, X. Chen, C. Dou. Observer-based event-triggered control for networked linear systems subject to denial-of-service attacks. *IEEE Transactions on Cybernetics*, vol. 50, pp. 1952-1964, 2020.

[22] X. Xie, Y. Liu, Q. Li. Neural networked-based adaptive event-triggered control for cyber-physical systems under resource constraints and hybrid cyberattacks. *Automatica*, vol. 152, Article 110977, 2023.

[23] M. Xue, H. Yan. H. Zhang, X. Zhan, K. Shi. Compensation-based output feedback control for fuzzy Markov jump systems with random packet losses. *IEEE Transactions on Cybernetics*, vol. 52, pp. 12759-12770, 2022.

[24] F. He, L. Wang, J. Wang, Y. Yao, D. Ji, W. Chen. A finite-time generalized H_2 gain measure and its performance criterion. *2013 9th Asian Control Conference (ASCC)*, 2013.

[25] Y. Bai, H.-J. Sun, A.-G. Wu. Finite-time stability and stabilization of Markovian jump linear systems subject to incomplete transition descriptions. *International Journal of Control, Automation and Systems*, vol. 19, pp. 2999–3012, 2021.

[26] S. Zhang, Y. Guo, S. Wang, Z. Liu, X. Hu. Finite-time bounded stabilisation for linear systems with finite-time H_2-gain constraint. *IET Control Theory & Applications*, vol. 14, pp. 1266-1275, 2020.

[27] X. Lv, Y. Niu, J. Song. Finite-time boundedness of uncertain Hamiltonian systems via sliding mode control approach. *Nonlinear Dynamics*, vol. 104, pp. 497–507, 2021.

[28] J. O. Baek, J. H. Park, Y. Gu. Event-triggered-based finite-time control of Markov jump systems. *2023 2nd International Conference on Machine Learinig, Control, and Robotics (MLCR)*, pp. 163-167, 2023.

[29] D. Yue, E. Tian, Q.-L. Han. A delay system method for designing event-triggered controllers of networked control systems. *IEEE Transactions on Automatic Control*, vol. 58, pp. 475–481, 2013.

[30] J. Liu, L. Wei, X. Xie, E. Tian, S. Fei. Quantized stabilization for T–S fuzzy systems with hybrid-triggered mechanism and stochastic cyber-attacks. *IEEE Transactions on Fuzzy Systems*, vol. 26, pp. 3820–3834, 2018.

[31] L. Yao, X. Huang, Z. Wang, H. Shen. Memory-based adaptive event-triggered control of Markov jump systems under hybrid cyber attacks: a switching-like adaptive law. *IEEE Transactions on Automation Science and Engineering*, vol. 21, pp. 6347-6357, 2024.

[32] J. Song, S. He. Finite-time robust optimal passive control for a class of uncertain nonlinear systems. *2013 The 25th Chinese Control and Decision Conference (CCDC)*, pp. 221-225, 2013.

[33] Y. Gu, Y. Shao, L. Li, M. Shen. Event-triggered fault tolerant control for Markov jump systems via a proportional-integral intermediate estimator. *Chaos, Solitons and Fractals*, vol. 180, 114553, 2024.